J|A|C|S ARTICLES

Published on Web 03/12/2009

Oxygen Ordering and Mobility in $YBaCo_4O_{7+\delta}$

Yan Jia,[†,⊥] Hua Jiang,[*,†] Markus Valkeapää,[‡] Hisao Yamauchi,[‡,§] Maarit Karppinen,[‡] and Esko I. Kauppinen[†,∥]

NanoMaterials Group, Department of Applied Physics and Center for New Materials, Helsinki University of Technology, P.O. Box 5100, FI-02015 TKK, Finland, Laboratory of Inorganic Chemistry, Department of Chemistry, Helsinki University of Technology, P.O. Box 6100, FI-02015 TKK, Finland, Materials and Structures Laboratory, Tokyo Institute of Technology, R3-3, 4249 Nagatsuta, Midori-ku, Yokohama 226-8503, Japan, and VTT Biotechnology, P.O. Box 1000, FI-02044 VTT, Finland

Received December 14, 2008; E-mail: hua.jiang@tkk.fi

Abstract: Extraordinary oxygen ordering and mobility have been found in an oxygen-nonstoichiometric mixed-valence cobalt oxide, $YBaCo_4O_{8.5}$. The excess oxygen atoms appear to be incorporated in an orderly way into the $YBaCo_4O_7$ parent lattice with different configurations as the oxygen content varies. Intense electron-beam irradiation was used to observe recurrent oxygen migration in the lattice, causing reversible structural modulation transitions. The oxygen migration can be attributed mainly to the electron-beam heating effect. This study highlights the high degree of freedom of surplus oxygen within the investigated structure and advances our understanding of the oxygen diffusion process in related transition-metal oxide systems.

Introduction

Since its discovery in 2002,[1] $YBaCo_4O_7$ has represented a model system on the basis of which a large number of its isomorphs have been developed through cation substitutions.[2−9] These emerging materials have displayed a rich variety of interesting physical and structural properties due to the rather unique Kagomé-type lattice and mixed-valence cobalt in their structures.[5−12] Moreover, $YBaCo_4O_7$ and its derivatives have also been found to exhibit great chemical flexibility, showing a large capacity for reversible oxygen absorption and desorption.[13−16] In general, $YBaCo_4O_7$ and its various derivatives constitute a new class of cobalt-based oxides denoted by $RBaCo_4O_{7+\delta}$ (R = rare-earth element), where the variable δ indicates oxygen nonstoichiometry.[13,15] Recently, by means of ultrahigh-pressure oxygenation treatment, a record-high oxygen content with $\delta \approx 1.56$ was achieved for $YBaCo_4O_{7+\delta}$,[17] indicating that its oxygen absorption capacity exceeds those reported for other oxide materials known to date. Hence, it stands out as a highly promising material for applications in oxygen storage, oxygen sensors, oxygen membranes, solid-oxide fuel cells, and so on.[14]

The remarkable physical properties and chemical flexibility of $YBaCo_4O_{7+\delta}$ are likely related to its uncommon crystal structure. X-ray diffraction (XRD) analysis indicated that the oxygen-stoichiometric $YBaCo_4O_7$ compound has a hexagonal ($P6_3mc$) structure with lattice parameters $a = 6.2982$ Å and $c = 10.2467$ Å ($c/a = 1.6269$)[1] that is built up of alternating stacking of Kagomé and triangular layers in a 3:1 ratio.[7,9,11] The structure is rather open and flexible, allowing it to accommodate appreciable numbers of excess oxygen atoms.[13] The extra oxygen was reported to cause the formation of a large superstructure, with an associated reduction in structural symmetry from hexagonal to orthorhombic.[18,19] Some possible models have been proposed to address where extra oxygen

[†] Department of Applied Physics and Center for New Materials, Helsinki University of Technology.
[‡] Department of Chemistry, Helsinki University of Technology.
[§] Tokyo Institute of Technology.
[∥] VTT Biotechnology.
[⊥] On leave from School of Physics, Northeast Normal University, Changchun 130024, China.

(1) Valldor, M.; Andersson, M. *Solid State Sci.* **2002**, *4*, 923.
(2) Valldor, M. *Solid State Sci.* **2004**, *6*, 251.
(3) Maignan, A.; Caignaert, V.; Pralong, V.; Pelloquin, D.; Hebert, S. *J. Solid State Chem.* **2008**, *181*, 1220.
(4) Tsipis, E. V.; Kharton, V. V.; Frade, J. R. *Solid State Ionics* **2006**, *177*, 1823.
(5) Maignan, A.; Caignaert, V.; Pelloquin, D.; Hebert, S.; Pralong, V.; Hejtmanek, J.; Khomskii, D. *Phys. Rev. B* **2006**, *74*, 165110.
(6) Valldor, M.; Hollmann, N.; Hemberger, J.; Mydosh, J. A. *Phys. Rev. B* **2008**, *78*, 024408.
(7) Markina, M.; Vasilchikova, T.; Vasiliev, A.; Lemmens, P.; Valldor, M. *J. Magn. Magn. Mater.* **2008**, *320*, e434.
(8) Nakayama, N.; Mizota, T.; Ueda, Y.; Sokolov, A. N.; Vasiliev, A. N. *J. Magn. Magn. Mater.* **2006**, *300*, 98.
(9) Huq, A.; Mitchell, J. F.; Zheng, H.; Chapon, L. C.; Radaelli, P. G.; Knight, K. S.; Stephens, P. W. *J. Solid State Chem.* **2006**, *179*, 1136.
(10) Soda, M.; Yasui, Y.; Moyoshi, T.; Sato, M.; Igawa, N.; Kakurai, K. *J. Phys. Soc. Jpn.* **2006**, *75*, 054707.
(11) Chapon, L. C.; Radaelli, P. G.; Zheng, H.; Mitchell, J. F. *Phys. Rev. B* **2006**, *74*, 172401.
(12) Tsipis, E. V.; Kharton, V. V.; Frade, J. R.; Nunez, P. *J. Solid State Electrochem.* **2005**, *9*, 547.
(13) Karppinen, M.; Yamauchi, H.; Otani, S.; Fujita, T.; Motohashi, T.; Huang, Y.-H.; Valkeapää, M.; Fjellvåg, H. *Chem. Mater.* **2006**, *18*, 490.
(14) Karppinen, M.; Yamauchi, H.; Fjellvåg, H.; Motohashi, T. Int. Pat. Appl. PCT/JP2006313436, filed June 6, 2006.
(15) Kadota, S.; Karppinen, M.; Motohashi, T.; Yamauchi, H. *Chem. Mater.* **2008**, *20*, 6378.
(16) Tsipis, E. V.; Khalyavin, D. D.; Shiryaev, S. V.; Redkina, K. S.; Nunez, P. *Mater. Chem. Phys.* **2005**, *92*, 33.
(17) Rasanen, S.; Yamauchi, H.; Karppinen, M. *Chem. Lett.* **2008**, *37*, 638.
(18) Valkeapää, M.; Karppinen, M.; Motohashi, T.; Liu, R. S.; Chen, J. M.; Yamauchi, H. *Chem. Lett.* **2007**, *36*, 1368.
(19) Chmaissem, O.; Zheng, H.; Huq, A.; Stephens, P. W.; Mitchell, J. F. *J. Solid State Chem.* **2008**, *181*, 664.

 10.1021/ja809745k CCC: $40.75 © **2009 American Chemical Society**

atoms might be accommodated.[12,19,20] In particular, Chmaissem et al.[19] have shown that if additional oxygen atoms are ordered in a doubled-superstructure unit cell to cause considerable displacements of several of the original oxygen atoms, a large orthorhombic superstructure ($a = 12.790$ Å, $b = 10.845$ Å, $c = 10.149$ Å) forms for $YBaCo_4O_{8.0}$ ($\delta = 1.0$) with respect to its parent $YBaCo_4O_7$ phase. Here we note that structural analysis of $RBaCo_4O_{7+\delta}$-type materials has to date been carried out mainly using X-ray or neutron powder diffraction.

Compared with X-ray or neutron diffraction, which gives only average structural information, the selected-area electron diffraction (SAED) technique allows the analysis of small individual crystal grains. Because light elements, such as oxygen, scatter electrons more effectively than X-rays, electron scattering techniques are considered more suitable for tracing oxygen. On the other hand, an electron beam can be used not only as the illumination source in an electron microscope but also as a tool to induce chemical reaction[21] or activate structural transitions.[22] In this work, we investigated the behavior of extra oxygen atoms in a highly oxygenated $YBaCo_4O_{8.5}$ sample by means of electron diffraction (ED). With the aid of ED analysis, we have shown the presence of extra oxygen in $YBaCo_4O_{8.5}$. The excess oxygen atoms are found to form ordering in various configurations, appearing as a number of structural modulations. In addition, by means of electron irradiation, we have observed an extraordinary phenomenon of oxygen mobility in $YBaCo_4O_{8.5}$. The recurrent migration of extra oxygen atoms in the lattice leads to reversible structural modulation transitions. On the basis of these findings, we give evidence for the high degree of freedom of extra oxygen in the $RBaCo_4O_{7+\delta}$-type structure, which is important for perceiving such a cobalt oxide system with a wide spectrum of oxygen-related properties.

Experimental Section

A $YBaCo_4O_{8.5}$ sample was synthesized by (*i*) a solid-state reaction at 1050 °C for 3 × 20 h of a mixture of Y_2O_3, $BaCO_3$, and Co_3O_4 powders in a stoichiometric ratio to form the parent phase $YBaCo_4O_7$, followed by (*ii*) oxygenation treatment of the as-prepared sample under an oxygen pressure of 10 MPa at 340 °C for 24 h. The oxygen content of the oxygenated sample was determined by iodometric titration to be $\delta = 1.5$.

ED experiments were carried out on a Philip CM200-FEG transmission electron microscope (TEM) operating at 200 kV and equipped with a side-entry ±40° double-tilt holder. Specimens for TEM observation were prepared by slightly milling the powder sample with ethanol in an agate mortar. A drop of the resulting suspension was cast onto a copper grid covered with holey carbon films. Small (~1 μm across) fragments of single-crystal grains supported on the carbon film (Figure S1 in the Supporting Information) were suitable for ED analysis.

Results

The crystal structure of the $YBaCo_4O_{8.5}$ sample was first characterized by XRD. A comparison with XRD data for $YBaCo_4O_{7+\delta}$ samples with different δ values[13,18,19] revealed that all of them have basically similar diffraction patterns with distinguishable features, indicating the fact of structural differences. However, XRD data are insufficiently sensitive to discriminate such differences in detail or may even be misleading if the structure is inhomogeneous. In the TEM, our ED analysis disclosed at least three different types of structure coexisting in the sample, hereafter called structures A, B, and C.

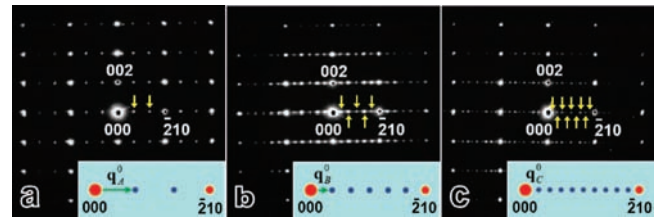

Figure 1. EDPs along the [120] zone axes of the three individual structures coexisting in $YBaCo_4O_{8.5}$: (a) structure A; (b) structure B; (c) structure C. The insets illustrate features of the structural modulation in each structure.

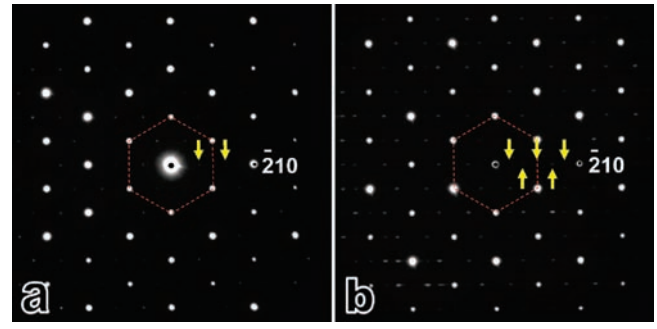

Figure 2. The [001]-incidence EDPs of (a) structure A and (b) structure B.

Figure 1 shows three ED patterns (EDPs) that were taken with the incident electron beam parallel to the [120] zone axes of the three structures A, B, and C. In addition to a set of main reflections that were indexed on the basis of the hexagonal lattice of the parent $YBaCo_4O_7$ phase, each EDP contains a large number of relatively weak spots regularly surrounding the main reflections as satellite spots. Thus, the structures are modulated. The features of the structural modulations are conventionally described by the modulation vector $\mathbf{q}$, as illustrated in the insets of Figure 1. The difference between the EDPs is noticeable. For structure A, the main diffraction vector $\mathbf{g}_{\bar{2}10}$ is equally divided into three parts by two satellite spots (indicated by arrows), and therefore, the modulation vector $\mathbf{q}_A^0 = (^1/_3)\mathbf{g}_{\bar{2}10}$. Likewise, $\mathbf{q}_B^0 = (^1/_6)\mathbf{g}_{\bar{2}10}$ for structure B, and $\mathbf{q}_C^0 = (^1/_{10})\mathbf{g}_{\bar{2}10}$ for structure C. Therefore, structure A has the shortest and structure C the longest modulation periodicity. The difference in the modulation frequencies is an indicator of the variable content of extra oxygen. The modulations for all three of the above structures appear along the [100] direction, normal to the $(\bar{2}10)$ lattice plane. Tilting the crystal of structure A in the microscope showed that the same modulation ($\mathbf{q}_A^0$) also appeared in two other equivalent directions, [010] and [110], and thus, the oxygen ordering did not break the hexagonal symmetry in structure A. This sixfold symmetry in modulated structure A is best viewed in the EDP of its [001] zone axis, which is presented in Figure 2a. However, for structure B, its [001]-incidence EDP (Figure 2b) indicates that the modulation $\mathbf{q}_B^0$ appears only along the [100] direction and not along its equivalent [010] and [110] directions, and thus, the structural symmetry was reduced. We have not yet succeeded in obtaining the [001]-incidence EDP of structure C. For the sake of comparison, we provide in Figure S2a in the Supporting Information the [001]-incidence EDP of

(20) Valldor, M. In *New Topics in Condensed Matter Research*; Chang, J. V., Ed.; Nova Science Publishers: New York, 2007; pp 75−102.
(21) Sun, L.; Banhart, F. *Appl. Phys. Lett.* **2006**, *88*, 193121.
(22) Zhan, Q.; Yu, R.; He, L. L.; Li, D. X.; Li, J.; Xu, S. Y.; Ong, C. K. *Phys. Rev. Lett.* **2002**, *88*, 196104.

the oxygen-stoichiometric $YBaCo_4O_7$ phase, which shows the sixfold symmetry but no features of structural modulation.

On the other hand, we noticed that the basic structures of all three of these phases, which are represented by the main reflections in the EDPs (Figures 1 and 2), are essentially the same, though they are slightly distorted from that of their parent $YBaCo_4O_7$ phase because of the excess oxygen introduced into the hexagonal lattice. After careful calibration, the lattice parameters *a* and *c* for the structures were measured from the respective panels of Figure 1. The results showed that the *a* values are nearly the same for all three structures [~6.29(5) Å], but the *c* values differ slightly from each other: 10.02(6), 10.05(0), and 10.08(3) Å for structures A, B, and C, respectively. From a comparison with the corresponding data measured for the parent $YBaCo_4O_7$ phase (Figure S2b in the Supporting Information), it is apparent that the *c* parameter is obviously shortened upon oxygen incorporation into the hexagonal lattice. Since the basic structure of $YBaCo_4O_{8.5}$ in fact does not significantly deviate from the parent hexagonal structure, the structural modulations are believed to be ascribed to ordering of the extra oxygen atoms. Considering the great difference in the modulation periodicities of the different structures, we believe that the oxygen content in the high-frequency modulated structure A is higher than that in the low-frequency modulated structure C. Because Co^{3+} is a smaller ion than Co^{2+},[23] the change in the oxidation state of cobalt from divalent to trivalent due to the introduction of extra oxygen into the lattice explains well the reduction in the unit-cell parameters in the oxygenated material and also accounts for the change in the *c* parameter over the different oxygen contents in structures A, B, and C. Here we remark that among the total number of observed grains in our experiments, there were six of structure A and five of structure B but only one of structure C.

As a result, we conclude that in the highly oxygenated compound $YBaCo_4O_{8.5}$, the excess oxygen atoms form several types of ordering, resulting in different structural modulations, probably with various excess oxygen content, and leading to changes in unit-cell size. It is worth underlining that the structural modulations remained rather stable in the TEM under the weak electron-beam illumination conditions (~0.02 A/cm^2) that were typically used for the low-magnification imaging observations and ED experiments.

However, using intense electron-beam irradiation, we observed remarkable phenomena of structural evolutions in $YBaCo_4O_{8.5}$ that behaved differently depending on the modulation type. Let us take structure A as an example. Upon irradiation of the same crystal for 2 min with an intense electron beam (~150 A/cm^2) along the [120] zone axis, the EDP features changed from those shown in Figure 1a to the ones appearing in Figure 3a, where the satellite reflections are so located to give the modulation vector $\mathbf{q}_A^I = (^1/_2)\mathbf{g}_{\bar{2}12}$ (Figure 3a, inset). After irradiation of the crystal for an additional 5 min, the location of the satellite spots changed again, resulting in a new type of structural modulation described by the modulation vector $\mathbf{q}_A^{II} = (^1/_3)\mathbf{g}_{\bar{2}10} + (^1/_2)\mathbf{g}_{002}$ (Figure 3b, inset). The dotted lines in Figure 3a,b schematically show the association of the satellite reflections with their corresponding main reflections. Before the modulation type $\mathbf{q}_A^{II}$ was completely formed, the transitional EDP shown in Figure 3c was recorded following irradiation for 2 min after Figure 3a was taken. Evidently, the modulations $\mathbf{q}_A^I$ and $\mathbf{q}_A^{II}$ coexist during the transitional stage.

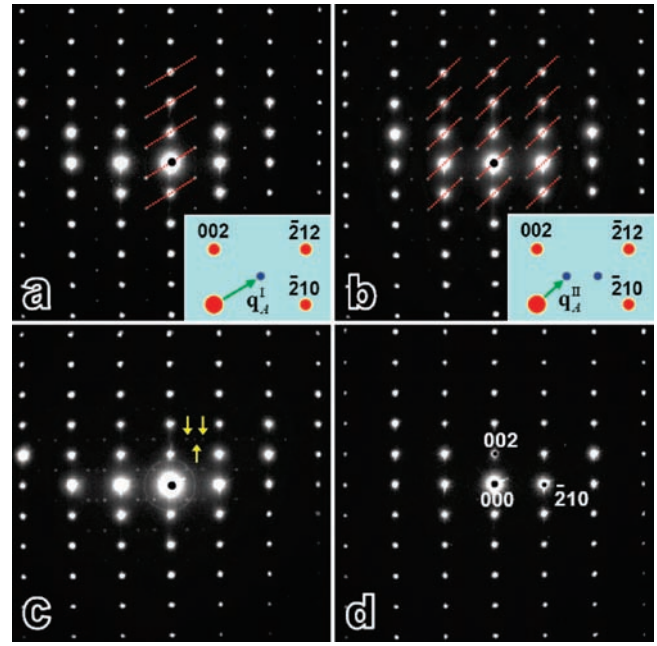

Figure 3. The [120]-incidence EDPs of structure A after intense electron-beam irradiation (~ 150 A/cm^2) for (a) 2, (b) 7, and (c) 4 min [an intermediate stage between (a) and (b)] and (d) ~5 h. In (a) and (b), the insets illustrate the modulation features, and the dotted lines schematically show the association of the satellite reflections with their corresponding main reflections.

Interestingly, with continuous electron-beam irradiation of the crystal, we observed that the structure modulations repeatedly changed back and forth between types $\mathbf{q}_A^I$ and $\mathbf{q}_A^{II}$. During an ~2 h irradiation experiment, the modulation transitions occurred eight times before modulation $\mathbf{q}_A^I$ stayed relatively stable for a long period (~3 h), after which the satellite reflections finally disappeared from the EDP, as shown in Figure 3d.

The structural modulation transitions were accompanied by noticeable changes in the lattice parameter *c* of the basic structure but no observable change in *a*, thus leading to a remarkable variation in the structural *c*/*a* ratio. From the original phase of structure A (Figure 1a), the *c*/*a* ratio was measured as $d_{002}/d_{\bar{2}10} = 1.59(3)$. After electron-beam irradiation, when the structure changed from $\mathbf{q}_A^I$ to $\mathbf{q}_A^{II}$, the corresponding *c*/*a* ratios increased to 1.61(8) for $\mathbf{q}_A^I$ and 1.62(4) for $\mathbf{q}_A^{II}$. When the modulation disappeared, the *c*/*a* ratio was measured using Figure 3d and turned out to be 1.62(6), which corresponds to the *c*/*a* ratio of the oxygen-stoichiometric $YBaCo_4O_7$ phase. On the basis of the above discussions, we can envisage that as a result of the intense electron-beam irradiation, excess oxygen atoms migrate within the structure to change the modulation from one type to another. The recurrent migration of extra oxygen atoms leads to reversible structural modulation transitions. In the transitional stage, most of the migrating oxygen atoms are not yet ordered, and thus, the satellite reflections in the EDP are relatively weak (Figure 3c). In the final stage, the system has released all of its extra oxygen in response to the long-time irradiation, thereby forming the oxygen-stoichiometric $YBaCo_4O_7$ phase.

It is interesting to remark that although the structural modulation repeatedly changed between $\mathbf{q}_A^I$ and $\mathbf{q}_A^{II}$ many times under electron-beam irradiation, the system never went back to its original state with $\mathbf{q}_A^0 = (^1/_3)\mathbf{g}_{\bar{2}10}$. A reasonable explanation for this is that when the original structure changed into the $\mathbf{q}_A^I$-

(23) Shannon, R. *Acta Crystallogr., Sect. A* **1976**, *32*, 751.

type modulation for the first time, the system released some of its extra oxygen atoms. In the subsequent structural transitions, there is insufficient oxygen content for the structure to return to its original shape.

Similar results were observed for structure B. However, for structure C we observed a different phenomenon when the crystal was irradiated using a similarly intense electron beam ($\sim$150 A/cm^2). With continuous irradiation, the structure modulation stayed as it was ($\mathbf{q}_C^0$) for $\sim$40 min with no observable change in its diffraction pattern and then suddenly transformed into the nonmodulated structure. This further demonstrates that the oxygen content plays a key role in the modulation transition. As we mentioned earlier, structure C has a long periodicity of modulation, and thus, the system preserves fewer extra oxygen atoms. As a result, it is unfavorable for structure C to form other types of modulation.

Discussion

It is an open question that is beyond the scope of this work to discuss how several different types of oxygen ordering were formed in the $YBaCo_4O_{8.5}$ material and related structures. Recent developments in spherical aberration (Cs)-corrected electron microscopy may provide an access to direct observation of oxygen and its mobility in the structure.[24] As for the mechanism of the oxygen migrations triggered by electron-beam irradiation, we consider the electron-beam heating effect as the main cause. Because of Coulomb interactions between the incoming electrons and the atomic electrons inside the specimen, appreciable energy can be transferred from the high incident energy and end up as heat within the specimen, giving rise to a local temperature increment of up to a few hundred degrees Celsius.[25] It has been reported that this temperature is suitable for an oxygen vacancy to migrate inside the lattice network of a layered transition-metal oxide.[26,27] Comparably, in our case, this is also a favorable temperature range around which $YBaCo_4O_{7+\delta}$ shows a reversible oxygen absorption/desorption property.[13] Besides the thermal conductivity property of the specimen, the incident electron energy and especially the beam current density are key factors in determining the local temperature increment. In the early stage of electron-beam irradiation, the local temperature of the sample stays within the oxygen-keeping limit (say, somewhat less than $\sim$400 °C) for the system to preserve the extra oxygen. The local temperature may vary because of frequent adjustments of beam current density for monitoring the evolution of the ED pattern. This may properly explain why the type of structural modulation changes back and forth in the beginning. Continuously irradiating the crystal for a certain period causes the local temperature to exceed the oxygen-keeping limit as a result of the accumulated heat in the sample, and thus, the system sharply releases its extra oxygen, eventually making the satellite reflections in the EDP disappear. The reversible oxygen mobility in $YBaCo_4O_{8.5}$ observed by ED is consistent with the results for the reversible oxygen absorption process reported by Karppinen and co-workers[13,15] and for reversible changes in conductivity and Seebeck coefficient reported by Tsipis and co-workers.[12,16]

Conclusions

To summarize, we have presented our discovery of extraordinary oxygen ordering and mobility phenomena in an emerging material, the oxygen-nonstoichiometric cobalt oxide $YBaCo_4O_{7+\delta}$. The surplus of oxygen has been shown to form several types of ordering in the parent lattice of $YBaCo_4O_7$, which appear as various structural modulations as the oxygen content varies. The structure may keep sixfold symmetry or take a lower symmetry, depending on the oxygen ordering type. Under intense electron-beam irradiation in a transmission electron microscope, extra oxygen atoms are found to recurrently migrate back and forth in the lattice to cause reversible structural modulation transitions. The oxygen migration can be mainly attributed to the electron-beam heating effect. This study highlights the high degree of freedom of excess oxygen within the investigated structure and advances the understanding of the oxygen diffusion process and oxygen-content-dependent physical properties in related transition-metal oxide systems.

Acknowledgment. This work was supported by the CNB-E Project of the TKK MIDE research program, the Finnish Government Scholarship (CIMO), the Academy of Finland (110433), Tekes (1726/31/07), and a Grant for R&D of New Interdisciplinary Fields in Nanotechnology and Materials Program of MEXT of Japan. We thank Samuli Räsänen for his help in the high-pressure oxygenation experiments and Dr. Paola Ayala for useful discussions in preparing the manuscript.

Supporting Information Available: Figures S1 and S2. This material is available free of charge via the Internet at http://pubs.acs.org.

JA809745K

(24) Urban, K. W. *Science* **2008**, *321*, 506.
(25) Chi, Z. H.; Yang, H.; Li, F. Y.; Yu, R. C.; Jin, C. Q.; Wang, X. H.; Deng, X. Y.; Li, L. T. *J. Phys: Condens. Matter* **2006**, *18*, 4371.
(26) Karppinen, M.; Yamauchi, H. In *Diverse Superconducting Systems and Some Miscellaneous Applications*; Narlikar, A. V., Ed.; Studies of High Temperature Superconductors, Vol. 37; Nova Science Publishers: New York, 2001; pp 109−143.
(27) van Doorn, R. H. E.; Burggraaf, A. J. *Solid State Ionics* **2000**, *128*, 65.